Biochimica et Biophysica Acta 1797 (2010) 197–203

Contents lists available at ScienceDirect

Biochimica et Biophysica Acta

journal homepage: www.elsevier.com/locate/bbabio

Patients with Leber hereditary optic neuropathy fail to compensate impaired oxidative phosphorylation

Alex Korsten [a], Irenaeus F.M. de Coo [a], Liesbeth Spruijt [c,1], L. Elly A. de Wit [b], Hubert J.M. Smeets [c], Wim Sluiter [a,*]

[a] Department of Neurology, Erasmus MC Rotterdam, The Netherlands
[b] Department of Biochemistry, Mitochondrial Research Unit, Erasmus MC Rotterdam, The Netherlands
[c] Genome Center, University of Maastricht, The Netherlands

ARTICLE INFO

Article history:
Received 3 August 2009
Received in revised form 7 October 2009
Accepted 8 October 2009
Available online 15 October 2009

Keywords:
Biochemical phenotype
Leber hereditary optic neuropathy
Mitochondrial density
Oxidative phosphorylation
Peripheral blood mononuclear cell

ABSTRACT

Ninety-five percent of Leber hereditary optic neuropathy (LHON) patients carry a mutation in one out of three mtDNA-encoded ND subunits of complex I. Penetrance is reduced and more male than female carriers are affected. To assess if a consistent biochemical phenotype is associated with LHON expression, complex I- and complex II-dependent adenosine triphosphate synthesis rates (CI-ATP, CII-ATP) were determined in digitonin-permeabilized peripheral blood mononuclear cells (PBMCs) of thirteen healthy controls and for each primary mutation of a minimum of three unrelated patients and of three unrelated carriers with normal vision and were normalized per mitochondrion (citrate synthase activity) or per cell (protein content). We found that in mitochondria, CI-ATP and CII-ATP were impaired irrespective of the primary LHON mutation and clinical expression. An increase in mitochondrial density per cell compensated for the dysfunctional mitochondria in LHON carriers but was insufficient to result in a normal biochemical phenotype in early-onset LHON patients.

1. Introduction

Leber hereditary optic neuropathy (LHON) is a mitochondrial genetic disorder characterized by a bilateral (sub)acute, painless optical atrophy occurring in previously healthy patients. More than 95% of the patients with LHON carry one of the three "primary" mtDNA mutations at position m.11778G>A, m.14484T>C, and m.3460G>A [1]. All three mutations occur in genes that encode the ND subunits of complex I (NADH:ubiquinone oxidoreductase, EC 1.6.5.3). Complex I is a large, multisubunit enzyme comprised of 7 mtDNA-encoded (ND1–ND6 and ND4L) and 38 nuclear-encoded polypeptides [2]. It removes electrons from NADH and passes them on to the electron acceptor ubiquinone. For each pair of electrons, four protons are transferred from the matrix across the inner membrane, which creates the electrochemical gradient that drives the synthesis of ATP from adenosine diphosphate and inorganic phosphate.

Biochemical data on mutation carriers and patients are only scarcely available and do not show a constant picture. Complex I activity measured in platelets, PBMC, lymphoblasts, EBV-transformed blood lymphocytes, and cybrids of affected and unaffected m.3460G>A carriers was reduced to 50–80%, whereas in m.11778G>A and m.14484T>C carriers, complex I activity is normal or only mildly reduced [3]. Complex I-dependent ATP production was decreased by 20% in leukocytes from four patients carrying the m.14488T>C mutation [4]. In lymphocytes from two patients carrying the m.11778G>A mutation, ATP synthesis decreased by about 50% using complex I substrates and by about 60% using complex II substrates [5]. In cybrids constructed by cell fusions of enucleated fibroblasts with rho° 206 cells from a total of six LHON patients harboring the m.3460G>A, m.11778G>A, or m.14484T>C mutation, complex I-dependent ATP synthesis was severely impaired (m.3460G>A and m.14484T>C more than 90% and m.11778G>A 65%), while complex II-dependent ATP synthesis was not affected [6].

LHON is characterized by strongly reduced penetrance. Approximately 30–50% of males and 10–20% of female LHON mutation carriers become symptomatic at a median age of 19 years (range 5–56 years) [7]. Apparently, the mtDNA mutation is necessary but not sufficient to induce the clinical expression of LHON [8]. Age and gender are the most important risk factors, although the underlying mechanism remains obscure, and thus far unidentified secondary genetic, epigenetic, and/or environmental might contribute to the variable expression of this disorder. In the present study, we investigated if a biochemical phenotype is associated with vision loss in primary LHON mutation carriers. As PBMCs represent an easily obtainable source of tissue that presents advantages over the use of fibroblasts or lymphoblast cell lines for research on oxidative

* Corresponding author. Department of Neurology, P.O. Box 2040, 3000 CA Rotterdam, The Netherlands. Tel.: +31 10 704 3335; fax: +31 10 704 4747.
E-mail address: w.sluiter@erasmusmc.nl (W. Sluiter).
[1] Present address: Department of Human Genetics, University Medical Centre, Nijmegen, The Netherlands.

0005-2728/$ – see front matter © 2009 Elsevier B.V. All rights reserved.
doi:10.1016/j.bbabio.2009.10.003

phosphorylation (OXPHOS) disorders [5], we performed our investigations on PBMC.

2. Materials and methods

2.1. Control subjects, carriers, and patients

The control group consisted of 13 subjects (6 males and 7 females, mean age 27.9 ± 4.1 years). The group with a LHON mtDNA mutation consisted of 26 unrelated subjects (15 males and 11 females, mean age 45.3 ± 19.7 years) of which 9 were carriers with normal vision (LHON−): m.3460G>A ($n=3$), m.11778G>A ($n=3$), and m.14484T>C ($n=3$) and 17 were visually impaired carriers (LHON+): m.3460G>A ($n=5$), m.11778G>A ($n=8$), and 14484T>C ($n=4$) (Table 1).

To minimize the chance that the LHON− group could be compromised by subjects who might be unaffected at the time of investigation but could lose their vision later in life, we only included unaffected carriers above the age at which the majority of the patients have become symptomatic. The peak age of LHON onset is between the age of 15 and 30 years and 95% of carriers who will experience visual failure (10–20% of the female carriers) will do so before the age of 50 years [9]. Therefore, only subjects with age ≥30 years were included in the LHON− group. All patient studies were performed as part of the diagnostic service, and therefore, approval of the ethical committee was not required. Patients (and controls) were informed according to hospital guidelines and Dutch legislation that residual material could be used for scientific research and they did not object.

2.2. Isolation, cryostorage, and thawing of peripheral blood mononuclear cells

Isolation of PBMCs from blood anti-coagulated with 0.18% EDTA has been described in detail elsewhere [10]. The cells were carefully resuspended in a small volume of (in mM) 250 sucrose, 10 HEPES (pH 7.4), and 1 EDTA (SHE).

Table 1
Characteristics of subjects.

LHON+	Gender	Mutation	Haplo group	Age	Age at onset
1	M	m.3460 G>A	J	21	20
2	M	m.3460 G>A	J	22	23
3	F	m.3460 G>A	H	40	15
4	M	m.3460 G>A	K	64	62
5	F	m.3460 G>A	H	73	16
6	M	m.11778 G>A	J	14	13
7	M	m.11778 G>A	H	19	19
8	M	m.11778 G>A	H	21	17
9	M	m.11778 G>A	H	46	36
10	M	m.11778 G>A	H	47	4
11	M	m.11778 G>A	H	49	34
12	M	m.11778 G>A	*	55	53
13	M	m.11778 G>A	T	61	56
14	M	m.14484 T>C	J	17	16
15	M	m.14484 T>C	J	28	23
16	M	m.14484 T>C	J	41	12
17	M	m.14484 T>C	*	60	49
LHON−	**Gender**	**Mutation**	**Haplo group**	**Age**	
1	F	m.3460 G>A	J	37	
2	F	m.3460 G>A	H	46	
3	F	m.3460 G>A	*	74	
4	F	m.11778 G>A	H	50	
5	F	m.11778 G>A	J	54	
6	F	m.11778 G>A	*	67	
7	F	m.14484 T>C	J	30	
8	F	m.14484 T>C	K	55	
9	F	m.14484 T>C	J	86	

For cryostorage, PBMCs were further diluted in RPMI containing 20% newborn calf serum (NBCS) to 20×10^6 cells/mL, kept for 30 min at 4 °C, after which an equal volume of ice-cold RPMI with 20% NBCS and 20% dimethyl sulfoxide was carefully added. Next, the cell suspension was transferred to 1-mL cryogenic vials in a Nalgene freezing container (Wessington Cryogenics), incubated overnight at −80 °C and stored in liquid nitrogen until use.

To study mitochondrial function, a cryovial with PBMCs was warmed rapidly by swirling in a 37 °C water bath. Immediately after thawing, the cells were washed three times with buffered saline (pH 7.4) containing 2 mM EDTA by centrifugation for 10 min at room temperature. Next, the cells were carefully resuspended and cell density adjusted to 10×10^6 cells/mL SHE. Cell viability was determined by trypan blue exclusion and ranged from 70% to 90%. A small sample was used to determine citrate synthase (CS) activity according to Srere [11] and protein concentration by the Bio-Rad DC protein assay (Bio-Rad Laboratories) with BSA as a standard. Complex I activity was determined according to de Wit and Sluiter [10] and complex II activity was measured by the method described by van Raam et al. [12].

2.3. ATP synthesis assay

The ATP production by PBMCs was determined essentially as described by Wanders et al. [13] for human skin fibroblasts by incubating 0.5×10^6 PBMCs/mL incubation medium consisting of 150 mM KCl, 25 mM Tris–HCl, 2 mM EDTA, 10 mM potassium phosphate buffer (pH 7.4), 10 μM ADP, 0.1% BSA, and 15 μg/mL digitonin in a 96-well black microplate (Optiplate; PerkinElmer) for 5 min at 37 °C to permeabilize the cells. As shown by Ouhabi et al. [14], the addition of EDTA to the incubation medium is necessary to prevent ATP hydrolysis by ATPase activities that are not lost during permeabilization. To investigate if 2 mM EDTA indeed inhibited these ATPase activities sufficiently during the ATP production assay, 1 μM ATP was added to some control and LHON PBMC samples, chosen at random, in the presence of 25 μM atractyloside to inhibit mitochondrial ATP synthesis. Under these conditions, not any statistically significant decrease in ATP concentration was demonstrable at various times during an incubation period of 10 min showing that all ATPase activities were blocked effectively. Consequently, the amount of ATP produced by control and LHON PBMCs will not decrease by simultaneous ATP hydrolysis. The complex I-dependent ATP production was assessed in the absence and presence of 0.5 μM of the specific complex I inhibitor rotenone, and started by adding 10 mM malate and 10 mM glutamate, and 0.6 mM malonate to inhibit any complex II activity. To assay ATP synthesis via complex II, the reaction was started by the addition of 10 mM succinate in the absence and presence of 100 mM of the competitive complex II inhibitor malonate, with 0.5 μM rotenone to prevent the formation of oxaloacetate that otherwise would inhibit complex II very strongly. Next, the microplate was gently shaken and incubated at 37 °C. After 30 min, the reaction was stopped by the addition of ATPLite (PerkinElmer) containing lucigenin and luciferase, the plate shaken, and next chemiluminescence measured by a TopCount NSX Scintillation Counter (PerkinElmer) using ATP as a standard. The net rate of complex I- and II-dependent ATP synthesis was calculated by subtraction of the rate in the presence of the respective specific complex I or II inhibitor from that in its absence. By assessing the ATP concentration at various times, control PBMCs were found to form ATP on glutamate/malate and on succinate as a statistically significant linear function of time up to 30 min of incubation ($R^2=0.9932$ and $P<0.001$; $R^2=0.9824$ and $P<0.001$). Therefore, the ATP synthesis rate was expressed as a single value in nanomoles of ATP synthesized per 30 min per milliunit of CS or per milligram of cell protein.

2.4. Blue native PAGE

Mitochondria were isolated from PBMCs and processed for two-dimensional blue native PAGE as previously described [12]. In short, after lysis by digitonin (4 g/g mitochondrial protein) 200 μg of mitochondrial protein was separated by BN-PAGE on a 5–13% acrylamide gradient gel. Strips from that first dimension were then excised, reduced for 1 hour at room temperature in 1% SDS containing 4 μL/mL tributylphosphine, and used for second dimension SDS–(12%) PAGE. After Western transfer onto a PVDF membrane using CAPS buffer (10 mM 3-[cyclohexylamino]-1-propane sulfonic acid, pH 11, 10% methanol), the cornerstone subunit of each of the five OXPHOS complexes were visualized with the OXPHOS Western blotting kit (MS601; Mitosciences), biotinylated anti-mouse IgG (RPN1001, Amersham Biosciences), streptavidin-biotinylated horseradish peroxidase complex (RPN1051; Amersham), and SuperSignal West Femto (Pierce). Images were acquired using a calibrated densitometer (GS-800; Bio-Rad) and the PDQuest software package (version 6.2.1; Bio-Rad).

2.5. Measurement of mitochondrial proton leak

To assess the magnitude of the proton leak the mitochondrial membrane potential ($\Delta\psi_m$) and state 2 respiration, defined as respiration in the presence of substrates without adenylates, was measured simultaneously in PBMCs from five controls and six LHON patients by a multisensor high-resolution respirometer (O2k-MiPNetAnalyzer; Oroboros Instruments) equipped with a tetraphenylphosphonium (TPP^+)-selective electrode filled with 10 mM TPP^+Cl^- and a 2-mm DriRef™ reference electrode (World Precision Instruments). Respirometric analysis was performed on-line using DatLab 4.3 software (Oroboros), and the rates of oxygen consumption were expressed as picomoles of O_2 per second per milligram of protein (pmol O_2 s^{-1} mg^{-1} protein). After a starvation period of 2 hours to increase the extremely low-PBMC oxygen consumption [12] by incubating $1.5–3.0\times10^6$ cells/mL at 37 °C under constant stirring (750 rpm) in proton leak buffer containing KCl (120 mM), KH_2PO_4 (3 mM), Tris (50 mM) and fatty acid-free BSA (0.25%, wt./vol.), pH 7.35, rotenone (5 μM), and oligomycin (1 μg/mL) were added, the PBMCs were permeabilized by 30 μg digitonin/10^6 cells, and the oxygen chamber was closed. After calibrating the TPP^+ electrode by successive additions of TPP^+ up to 1.5 μM using a titration-injection micropump (Oroboros), the PBMC mitochondria were energized by the addition of 2.5 mM succinate. Unfortunately, accurate titration of the still low oxygen consumption rate with malonate was impossible. Instead, 1 μM carbonyl cyanide *p*-trifluoromethoxyphenylhydrazone was added to release TPP^+ for baseline correction. The calculation of $\Delta\psi_m$ was obtained from the Nernst equation using a TPP^+-binding mean correction factor of 0.13 [15], and an estimated intra-mitochondrial volume of 1 μL/mg of protein [16].

2.6. Statistical analysis

Statistical analyses were performed with Stata/SE 10.1 software (StataCorp LP, College Station, TX). The results were expressed as the mean ± standard deviation (SD). Skewness/kurtosis tests for normality showed that the data obtained for CI-ATP per milliunit of CS and CI-ATP per milligram of protein were normally distributed and for mitochondrial density, CII-ATP per milliunit of CS, and CII-ATP per milligram of protein after natural logarithm transformation. Differences between groups were then evaluated on the basis of Student's *t*-test or one-way analysis of variance where appropriate. When significant *F* values were obtained, individual group means were tested for differences according to Bonferroni's *a posteriori* correction for multiple comparisons. The criterion for significance was $P<0.05$ for all comparisons.

As a consequence of the fact that more male than female carriers are affected, our goal to classify the LHON mutation carriers based on the clinical expression of the disease, i.e., into a group of LHON patients and a group of carriers without vision loss, implies a strong bias on gender. Therefore, any analysis on gender is meaningless.

Linear regression analyses of CI-ATP and CII-ATP per milliunit of CS on age indicated a marginal ($R^2=0.20$) but significant ($P<0.005$) age effect that was lost after patient 9 of the LHON− group (86 years of age) was omitted from the database. Therefore, that patient was not taken into further account.

To examine if early- and late LHON+ differ in their ability to compensate per cell for the impaired mitochondrial-dependent ATP synthesis, a Kruskall–Wallis equality-of-populations rank test and a two-sample Kolmogorov–Smirnov test for equality-of-distribution functions were performed after assigning the distinction "positive" to values of CI-ATP per milligram of protein that were equal or higher than the lowest control value and else "negative."

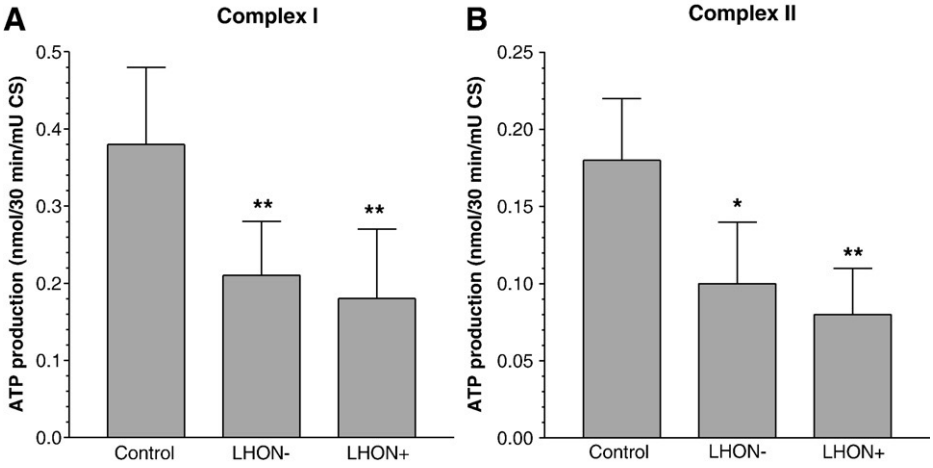

Fig. 1. Comparison of the rates of complex I- (A) and complex II-dependent (B) ATP synthesis of PBMC mitochondria between controls, LHON− and LHON+. The ATP production was determined by incubating 0.5×10^6 PBMC per milliliter of incubation medium containing 2 mM EDTA to inhibit ATPase activities during 30 min in the presence of 10 mM glutamate/malate and 0.6 mM malonate to inhibit complex II with or without 0.5 μM rotenone (CI-ATP), or of 10 mM succinate and 0.5 μM rotenone with or without 100 mM malonate (CII-ATP). The ATP concentration at the end of incubation period was assessed by the ATPLite 1step assay of PerkinElmer (Zaventem, Belgium). The net CI-ATP and CII-ATP was calculated by subtracting the ATP concentration in the presence of the respective specific inhibitor from that in its absence and expressed as nanomoles of ATP/30 min/mU citrate synthase (CS). Data are expressed as the mean ± SD. $^*P<0.05$ and $^{**}P<0.001$ versus control.

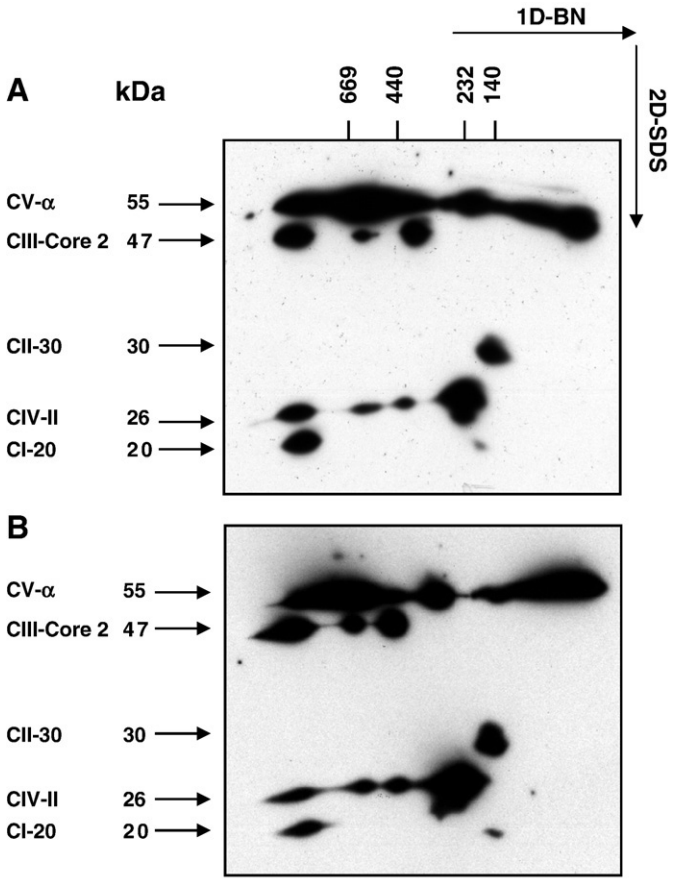

Fig. 2. Supercomplex organization of OXPHOS complexes in PBMC mitochondria from a control (A) and a LHON mutation carrier (B). After solubilization of equal amounts of mitochondrial membranes with digitonin, supercomplex separation was achieved by 1D blue native electrophoresis followed by 2D SDS–PAGE to resolve the composition of each of the supercomplexes. The cornerstone subunits of each of the five OXPHOS complexes were visualized with the OXPHOS Western blotting kit (MS601; Mitosciences), biotinylated anti-mouse IgG (RPN1001, Amersham Biosciences), streptavidin-biotinylated horseradish peroxidase complex (RPN1051; Amersham) and SuperSignal West Femto (Pierce). Images were acquired using a calibrated densitometer (GS-800; Bio-Rad) and the PDQuest software package (version 6.2.1; Bio-Rad).

3. Results

3.1. Complex I- and II-dependent ATP production is decreased in mitochondria of LHON mutation carriers

To find out if mitochondrial function of LHON PBMC differed from controls, the rate of ATP synthesis was assessed. The rates of ATP synthesis driven by malate/glutamate (CI-ATP) and by succinate (CII-ATP) were determined and normalized for CS activity. To prevent a family-based bias in this study, we only included LHON mutation carriers and patients who were unrelated. Obviously, this stringent criterion limited the number of patients that could be included into the study and unfortunately led to a stronger than usual bias on sex. The affected group (LHON+) consisted of 88.2% males, and in the unaffected group (LHON−), all subjects were female (Table 1). In our previous studies [17–19], we found that 74.5% of the affected subjects were male, and conversely, of the unaffected subjects, 70.9% were female. Undoubtedly, due to the stringent inclusion criterion and the fact that only 46 LHON families were available in the Netherlands, no unaffected male LHON mutation carriers were included into the present study. We found that CI-ATP per mitochondrion in the LHON+ and LHON− group was 53% ($P<0.001$) and 45% ($P<0.001$), respectively, lower than in the control group (0.38 ± 0.10 nmol/30 min/mU CS) (Fig. 1A).

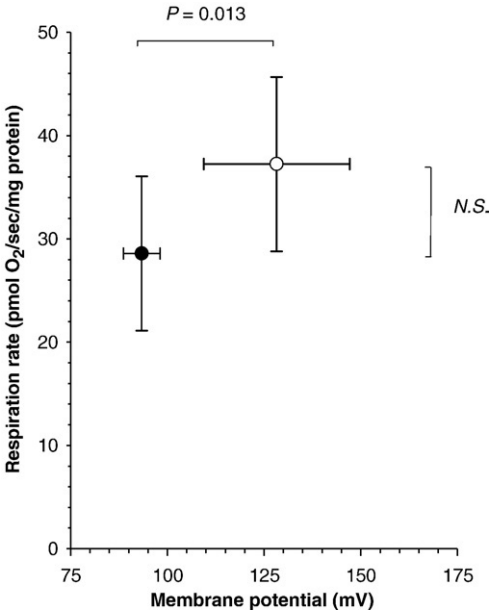

Fig. 3. Respiration-driven proton leak in PBMC from control (○) ($n=5$) and LHON (●) ($n=6$) subjects. The mitochondrial membrane potential (mV) and state 2 respiration rate (pmol O_2 per sec and per mg protein) achieved by addition of 2.5 mM succinate in the absence of adenylates were measured simultaneously in $1.5–3.0 \times 10^6$ digitonin-permeabilized PBMC per milliliter of proton leak buffer consisting of KCl (120 mM), KH_2PO_4 (3 mM), Tris (50 mM) and fatty acid-free BSA (0.25%, wt./vol.), pH 7.35, rotenone (5 μM), and oligomycin (1 μg/mL) in a multisensor high-resolution respirometer (Oroboros Instruments, Innsbruck, Austria) using tetraphenylphosphonium-selective electrodes. Data are expressed as the mean ± SD.

CII-ATP per mitochondrion of LHON+ PBMC was 57% lower ($P<0.001$) and of LHON− 42% lower ($P=0.012$) than controls (0.18 ± 0.04 nmol/30 min/mU CS) (Fig. 1B). There was no statistically significant difference between LHON+ and LHON− regarding CI-ATP and CII-ATP per mitochondrion. The coefficient of intra-assay variation of the ATP synthesis measurements ranged between 6% and 8%.

3.2. Supercomplex expression in PBMC mitochondria is not different between control and LHON

It is surprising that a defect in complex I caused by an mtDNA mutation in LHON has led to an impaired complex II-dependent ATP

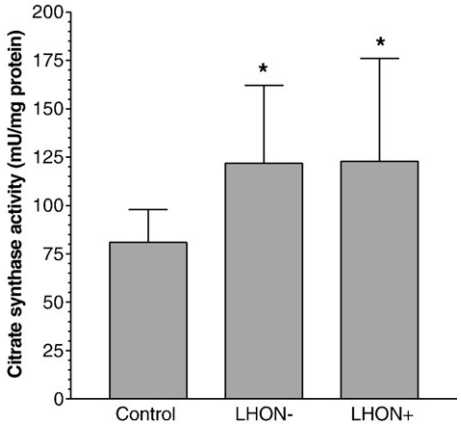

Fig. 4. Mitochondrial density of PBMC from controls ($n=12$), LHON− ($n=8$), and LHON+ ($n=17$) as reflected by the expression of the mitochondrial matrix enzyme citrate synthase (CS) expressed as milliunits of CS per milligram of cell protein. Data represent the mean ± SD. *$P<0.05$ versus control.

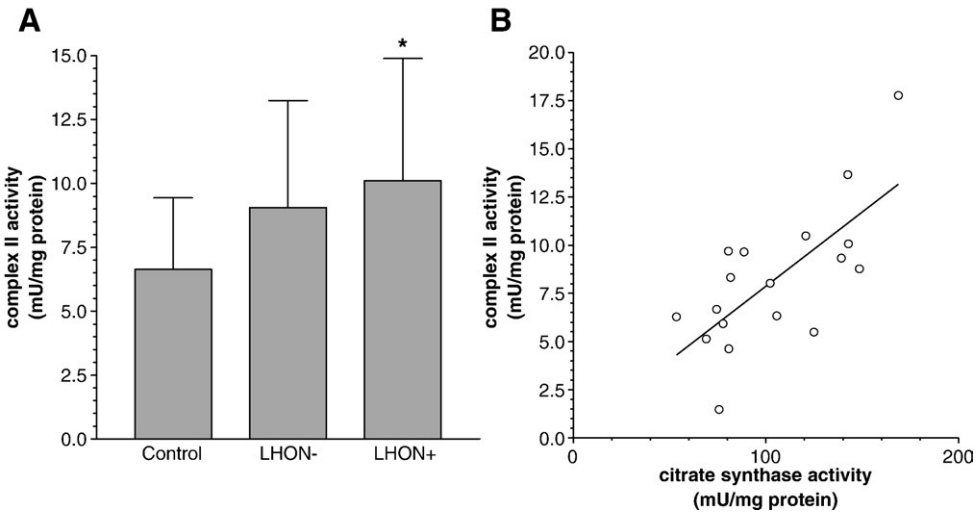

Fig. 5. Mitochondrial density of PBMC from controls ($n=10$), LHON− ($n=3$), and LHON+ ($n=5$) as reflected by the expression of the mitochondrial inner membrane enzyme complex II expressed as milliunits per milligram of cell protein (A) and the association of citrate synthase activity with the amount of complex II activity (B). $^{*}P<0.05$ versus control.

synthesis. Since formation of a supercomplex consisting of complex I, III, and IV appears essential for effective energy generation [20] and any change in its composition and level of expression may interfere with CII-ATP (via available complex III and IV) as well, we studied if the expression of complex II and this process was impaired due to the mutation in complex I explaining the impaired CI-ATP and CII-ATP. Based on the known molecular masses of the OXPHOS complexes [20], 2D BN-PAGE of equal amounts of mitochondria showed that both in control (Fig. 2A) and in LHON PBMC (Fig. 2B), the majority of complex I apparently is bound to complex III and IV into a large supercomplex of ~1.5 MDa. The supercomplex did not differ in composition and in magnitude of expression between control and LHON PBMC mitochondria. The faint spot with a molecular mass in-between 140-232 kDa might represent a complex I subcomplex [21]. Complex II was found as a monomer (~140 kDa) only and the expression level was comparable between control and LHON PBMC mitochondria (Fig. 2A and B).

3.3. Proton leak is higher in LHON PBMC mitochondria

Recent data have shown that LHON fibroblasts may share a common mitochondrial coupling defect with other hereditary optic neuropathies [22]. To establish if this is also the case in LHON PBMC as an explanation for the decreased CII-ATP, the respiration-driven proton leak in control and LHON PBMC mitochondria was assessed. Fig. 3 shows that the mitochondrial membrane potential of LHON PBMC mitochondria was significantly ($P=0.013$) lower than that of control mitochondria. The oxygen consumption rates were not significantly different.

3.4. Mitochondrial density is increased in LHON mutation carriers

To study if the impaired respiratory chain-dependent ATP synthesis by LHON+ and LHON− mitochondria might be compensated by an increase in mitochondrial density, the amount of CS activity of LHON and control PBMC serving as a marker for mitochondrial mass [11,23] was determined. Mitochondrial density was 53% higher ($P=0.016$) in LHON+ and 52% higher ($P=0.044$) in LHON− compared to controls (81 ± 17 mU CS/mg protein) (Fig. 4).

To reinforce the finding that mitochondrial density increased in LHON mutation carriers and patients compared to controls, we assessed the relationship between the level of expression of citrate synthase, a marker of the mitochondrial matrix, and complex II as a marker of the mitochondrial inner membrane, in a number of control, LHON−, and LHON+ samples as well. We found higher complex II levels in the two LHON groups compared to the control group (Fig.

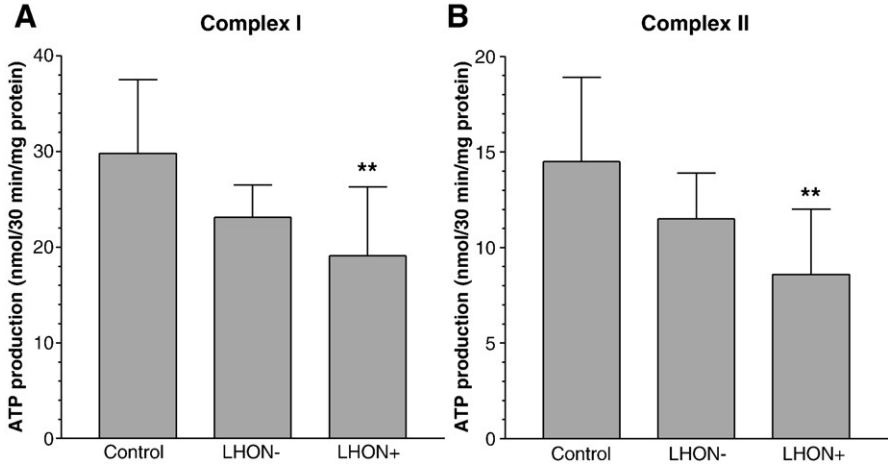

Fig. 6. Complex I- (A) and complex II-dependent (B) ATP synthesis rates of control, LHON−, and LHON+ PBMC expressed as nanomoles of ATP/30 min/mg protein. See the legend of Fig. 1 for further details of the ATP synthesis assay. Data represent the mean ± SD. $^{**}P<0.001$ versus control.

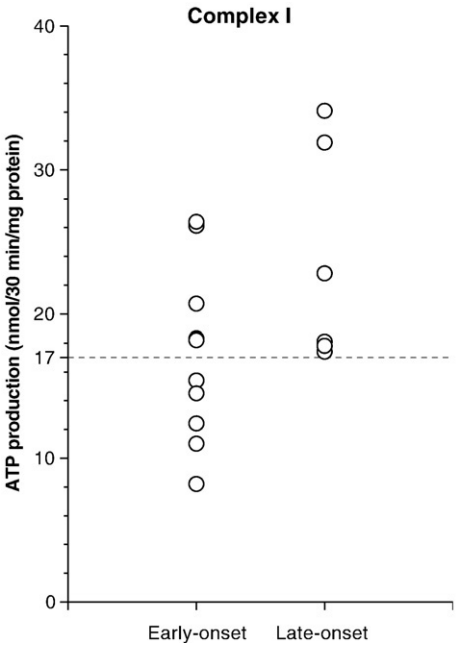

Fig. 7. Complex I-dependent ATP synthesis rates of PBMC from early-onset (≤24 years) and late-onset (>24 years) LHON+ patients expressed as nanomoles of ATP/30 min/mg protein. See the legend of Fig. 1 for further details of the ATP synthesis assay. Individual data are shown; the dashed line representing the lowest normal value.

5A), and a statistically significant linear relationship between these two markers ($R^2 = 0.501$, $P < 0.001$, $n = 18$) (Fig. 5B).

3.5. Increased mitochondrial density per cell compensates reduced ATP production per mitochondrion in carriers but not in LHON patients

To examine if the increase in mitochondrial density in PBMC of LHON carriers and patients compensated the impaired rate of mitochondrial-dependent ATP synthesis, we determined the ATP synthesis rate per milligram of cell protein. Indeed, in LHON−, CI-ATP per cell did not differ significantly (22% lower, $P = 0.11$) from controls (29.8 ± 7.7 nmol/30 min/mg protein), but in LHON+, CI-ATP per cell was still 36% lower ($P < 0.001$) than controls (Fig. 6A). Moreover, in the LHON+ group, early-onset (≤24 years) LHON PBMC had a significantly ($P = 0.03$) lower ability than late-onset (>24 years) LHON PBMC to synthesize ATP via complex I at least at the lowest normal rate of 17 nmol ATP/30 min/mg protein (Fig. 7).

CII-ATP per cell was 41% lower ($P = 0.002$) in LHON+, but in LHON−, it was not significantly lower (21%, $P = 0.36$) than in controls (14.5 ± 4.4 nmol/30 min/mg protein) (Fig. 6B).

4. Discussion

The results of this study showed that in concurrence with previous reports [4–6], CI-ATP by mitochondria of LHON mutation carriers was impaired and that dysfunction of OXPHOS in LHON can be detected using peripheral blood mononuclear cells. Furthermore, the results showed that despite defective mitochondrial CI-ATP and CII-ATP, OXPHOS-dependent ATP production *per cell* is not significantly impaired in unaffected LHON carriers.

Although impaired CI-ATP by PBMC mitochondria of LHON mutation carriers could be explained by a dysfunctional complex I due to the mutated ND gene, we found that complex I enzyme activity of PBMC of five LHON+ and four LHON− determined *in vitro* did not differ statistically significantly from controls (expressed as milliunit of complex I activity per unit of citrate synthase activity, the means (and SD) amounted to 48.7 (23.5), 43.7 (13.4), and 48.4 (19.4), respectively). Previously, Brown et al. [24] reported varying outcomes of complex I activity in LHON as well. This discrepancy between the *in vitro* and *in situ* situation could be due to the fact that complex I activity *in vitro* is determined under optimal conditions, e.g., under saturating substrate concentrations, and that most spectrophotometric assays are not directed to detect a defective proton translocation. Importantly, that exemplifies the relevance of *in vivo* measurements.

Our results not only showed impaired CI-ATP by PBMC mitochondria of LHON carriers and patients but also impaired CII-ATP. This is different to the findings of Baracca et al. [6] in LHON cybrids, showing only impaired CI-ATP per cell. Because complex II is encoded by nuclear genes [25] and the primary LHON mutations are located in mtDNA, only a common mechanism can explain the combined impaired CI-ATP and CII-ATP of LHON PBMC mitochondria. Based on our measurements of the mitochondrial membrane potential during state 2 respiration, we postulate an increased proton leak in PBMC mitochondria of LHON mutation carriers, suggesting that the decreased CII-ATP by PBMC mitochondria is a *secondary* phenomenon resulting from a dysfunctional complex I in those cells. Apparently, that phenomenon did not occur in freshly cultured LHON cybrids and might need time to become effective [6]. Superoxide can damage the mitochondrial inner membrane through the formation of peroxynitrite promoting proton leak [26]. Although it is still under debate which is the exact site at complex I where superoxide is generated [27], the levels of this reactive oxygen species (ROS) increase when complex I does not function properly [28,29]. Indeed, the levels of ROS in LHON mitochondria are higher than normal [30,31].

We have found that the mitochondrial density in PBMC of mutation carriers irrespective of the clinical status was higher than in healthy controls. Recently, in non-arteritic anterior ischaemic optic neuropathy such a phenomenon has been reported as well [32]. If mitochondria are no longer capable of meeting cellular ATP demand, via a complex signal transduction pathway involving AMP-activated protein kinase [33] and the master switch, peroxisome proliferator-activated receptor gamma coactivator 1α [34], the number of mitochondria as a compensation will finally increase. Despite the increased mitochondrial density, our data showed that this was not sufficient to effectively restore the cellular CI-ATP and CII-ATP in the group of LHON patients (LHON+). In that respect, especially, a subgroup of patients who lost their vision before the age of 24 years was significantly less successful than their counterparts who lost vision later in life. A population-based clinical study of LHON in the North East of England determined that 75% of LHON+ was younger than 24 years [7], which might point out a fundamental difference in etiology between early-onset LHON+ (age ≤24 years) and late-onset LHON+ (age >24 years). The absence of a protective genetic modifier or the presence of a risk factor could contribute to the early-onset in those patients.

In conclusion, we have shown that, in LHON mutation carriers, but not in (early-onset) LHON patients, an increase in mitochondrial density in PBMC fully compensated per cell the impaired CI-ATP and CII-ATP. This provides a biochemical phenotype that might be useful for prognostic predictions in mutation carriers and this subphenotype may also help to identify new LHON modifier genes in families. Our data indicate that such a gene may be involved in mitochondrial biogenesis.

Acknowledgements

This work was supported by the MITOCIRCLE project, a Specific Targeted Research Project co-funded by the Sixth Research Framework Programme of the European Union (contr. no. 005260).

We thank all the patients and their family members and the "LOA"-patient organisation (Eindhoven) for their participation in this study.

References

[1] D.A. Mackey, R.J. Oostra, T. Rosenberg, E. Nikoskelainen, J. Bronte-Stewart, J. Poulton, A.E. Harding, G. Govan, P.A. Bolhuis, S. Norby, Primary pathogenic mtDNA mutations in multigeneration pedigrees with Leber hereditary optic neuropathy, Am. J. Hum. Genet. 59 (1996) 481–485.

[2] J. Carroll, I.M. Fearnley, J.M. Skehel, R.J. Shannon, J. Hirst, J.E. Walker, Bovine complex I is a complex of 45 different subunits, J. Biol. Chem. 281 (2006) 32724–32727.

[3] M.D. Brown, The enigmatic relationship between mitochondrial dysfunction and Leber's hereditary optic neuropathy, J. Neurol. Sci. 165 (1999) 1–5.

[4] R.J. Oostra, M.J. Van Galen, P.A. Bolhuis, E.M. Bleeker-Wagemakers, C. Van den Bogert, The mitochondrial DNA mutation ND6*14,484C associated with Leber hereditary optic neuropathy, leads to deficiency of complex I of the respiratory chain, Biochem. Biophys. Res. Commun. 215 (1995) 1001–1005.

[5] B.J. Marriage, M.T. Clandinin, I.M. MacDonald, D.M. Glerum, The use of lymphocytes to screen for oxidative phosphorylation disorders, Anal. Biochem. 313 (2003) 137–144.

[6] A. Baracca, G. Solaini, G. Sgarbi, G. Lenaz, A. Baruzzi, A.H.V. Schapira, A. Martinuzzi, V. Carelli, Severe impairment of complex I-driven adenosine triphosphate synthesis in Leber hereditary optic neuropathy cybrids, Arch. Neurol. 62 (2005) 730–736.

[7] P. Yu-Wai-Man, P.G. Griffiths, D.T. Brown, N. Howell, D.M. Turnbull, P.F. Chinnery, The epidemiology of Leber hereditary optic neuropathy in the North East of England, Am. J. Hum. Genet. 72 (2003) 333–339.

[8] M.Y. Yen, A.G. Wang, Y.H. Wei, Leber's hereditary optic neuropathy: a multifactorial disease, Prog. Retin. Eye Res. 25 (2006) 381–396.

[9] P. Yu-Wai-Man, P.G. Griffiths, G. Hudson, P.F. Chinnery, Inherited mitochondrial optic neuropathies, J. Med. Genet. 46 (2009) 145–158.

[10] L.E.A. de Wit, W. Sluiter, Reliable assay for measuring complex I activity in human blood lymphocytes and skin fibroblasts, Methods Enzymol. 456 (2009) 169–181.

[11] P.A. Srere, Citrate synthase, Methods Enzymol. 13 (1969) 3–11.

[12] B.J. van Raam, W. Sluiter, L.E.A. de Wit, D. Roos, A.J. Verhoeven, T.W. Kuijpers, Mitochondrial membrane potential in human neutrophils is maintained by complex III activity in the absence of supercomplex organisation, PLoS ONE 3 (2008) e2013.

[13] R.J.A. Wanders, J.P.N. Ruiter, F.A. Wijburg, Studies on mitochondrial oxidative phosphorylation in permeabilized human skin fibroblasts: application to mitochondrial encephalomyopathies, Biochim. Biophys. Acta 1181 (1993) 219–222.

[14] R. Ouhabi, M. Boue-Grabot, J.P. Mazat, Mitochondrial ATP synthesis in permeabilized cells: assessment of the ATP/O values in situ, Anal. Biochem. 263 (1998) 169–175.

[15] M. Demura, N. Kamo, Y. Kobatake, Mitochondrial membrane potential estimated with the correction of probe binding, Biochim. Biophys. Acta 894 (1987) 355–364.

[16] M.D. Brand, S.M. Felber, Membrane potential of mitochondria in intact lymphocytes during early mitogenic stimulation, Biochem. J. 217 (1984) 453–459.

[17] G. Hudson, V. Carelli, L. Spruijt, M. Gerards, C. Mowbray, A. Achilli, A. Pyle, J. Elson, N. Howell, C. La Morgia, M.L. Valentino, K. Huoponen, M.L. Savontaus, E. Nikoskelainen, A.A. Sadun, S.R. Salomao, R. Belfort Jr., P. Griffiths, P. Yu-Wai-Man, I.F.M. de Coo, R. Horvath, M. Zeviani, H.J.M. Smeets, A. Torroni, P.F. Chinnery, Clinical expression of Leber hereditary optic neuropathy is affected by the mitochondrial DNA-haplogroup background, Am. J. Hum. Genet. 81 (2007) 228–233.

[18] M.A. Kirkman, A. Korsten, M. Leonhardt, K. Dimitriadis, I.F.M. De Coo, T. Klopstock, P.G. Griffiths, G. Hudson, P.F. Chinnery, P. Yu-Wai-Man, Quality of life in patients with Leber hereditary optic neuropathy, Invest. Ophthalmol. Vis. Sci. 50 (2009) 3112–3115.

[19] M.A. Kirkman, P. Yu-Wai-Man, A. Korsten, M. Leonhardt, K. Dimitriadis, I.F.M. De Coo, T. Klopstock, P.F. Chinnery, Gene–environment interactions in Leber hereditary optic neuropathy, Brain 132 (2009) 2317–2326.

[20] M. D'Aurelio, C.D. Gajewski, G. Lenaz, G. Manfredi, Respiratory chain supercomplexes set the threshold for respiration defects in human mtDNA mutant cybrids, Hum. Mol. Genet. 15 (2006) 2157–2169.

[21] H. Antonicka, I. Ogilvie, T. Taivassalo, R.P. Anitori, R.G. Haller, J. Vissing, N.G. Kennaway, E.A. Shoubridge, Identification and characterization of a common set of complex I assembly intermediates in mitochondria from patients with complex I deficiency, J. Biol. Chem. 278 (2003) 43081–43088.

[22] A. Chevrollier, V. Guillet, D. Loiseau, N. Gueguen, M.A. de Crescenzo, C. Verny, M.F. Eng, H. Dollfus, S. Odent, D. Milea, C. Goizet, P. Amati-Bonneau, V. Procaccio, D. Bonneau, P. Reynier, Hereditary optic neuropathies share a common mitochondrial coupling defect, Ann. Neurol. 63 (2008) 794–798.

[23] K. Renner, A. Amberger, G. Konwalinka, R. Kofler, E. Gnaiger, Changes of mitochondrial respiration, mitochondrial content and cell size after induction of apoptosis in leukemia cells, Biochim. Biophys. Acta 1642 (2003) 115–123.

[24] M.D. Brown, I.A. Trounce, A.S. Jun, J.C. Allen, D.C. Wallace, Functional analysis of lymphoblast and cybrid mitochondria containing the 3460, 11778, or 14484 Leber's hereditary optic neuropathy mitochondrial DNA mutation, J. Biol. Chem. 275 (2000) 39831–39836.

[25] G. Burger, B.F. Lang, M. Reith, M.W. Gray, Genes encoding the same three subunits of respiratory complex II are present in the mitochondrial DNA of two phylogenetically distant eukaryotes, Proc. Natl. Acad. Sci. U.S.A. 93 (1996) 2328–2332.

[26] P.S. Brookes, J.M. Land, J.B. Clark, S.J. Heales, Peroxynitrite and brain mitochondria: evidence for increased proton leak, J. Neurochem. 70 (1998) 2195–2202.

[27] G. Lenaz, A. Baracca, R. Fato, M.L. Genova, G. Solaini, Mitochondrial complex I: structure, function, and implications in neurodegeneration, Ital. J. Biochem. 55 (2006) 232–253.

[28] S. Verkaart, W.J. Koopman, S.E. van Emst-de Vries, L.G. Nijtmans, L.W. van den Heuvel, J.A. Smeitink, P.H. Willems, Superoxide production is inversely related to complex I activity in inherited complex I deficiency, Biochim. Biophys. Acta 1772 (2007) 373–381.

[29] K. Ishikawa, K. Takenaga, M. Akimoto, N. Koshikawa, A. Yamaguchi, H. Imanishi, K. Nakada, Y. Honma, J. Hayashi, ROS-generating, mitochondrial DNA mutations can regulate tumor cell metastasis, Science 320 (2008) 661–664.

[30] V. Carelli, A. Ghelli, M. Ratta, E. Bacchilega, S. Sangiorgi, R. Mancini, V. Leuzzi, P. Cortelli, P. Montagna, E. Lugaresi, M. Degli Esposti, Leber's hereditary optic neuropathy: biochemical effect of 11778/ND4 and 3460/ND1 mutations and correlation with the mitochondrial genotype, Neurology 48 (1997) 1623–1632.

[31] V. Carelli, A. Ghelli, L. Bucchi, P. Montagna, A. De Negri, V. Leuzzi, C. Carducci, G. Lenaz, E. Lugaresi, M. Degli Esposti, Biochemical features of mtDNA 14484 (ND6/M64V) point mutation associated with Leber's hereditary optic neuropathy, Ann. Neurol. 45 (1999) 320–328.

[32] K.K. Abu-Amero, T.M. Bosley, Increased relative mitochondrial DNA content in leucocytes of patients with NAION, Br. J. Ophthalmol. 90 (2006) 823–825.

[33] R.M. Reznick, G.I. Shulman, The role of AMP-activated protein kinase in mitochondrial biogenesis, J. Physiol. 574 (2006) 33–39.

[34] Z. Wu, P. Puigserver, U. Andersson, C. Zhang, G. Adelmant, V. Mootha, A. Troy, S. Cinti, B. Lowell, R.C. Scarpulla, B.M. Spiegelman, Mechanisms controlling mitochondrial biogenesis and respiration through the thermogenic coactivator PGC-1, Cell 98 (1999) 115–124.